ISSN 1063-780X, Plasma Physics Reports, 2022, Vol. 48, No. 10, pp. 1116–1123. © The Author(s), 2022. This article is an open access publication.
Russian Text © The Author(s), 2022, published in Fizika Plazmy, 2022, Vol. 48, No. 10, pp. 967–974.

NONLINEAR STRUCTURES

Influence of Ion–Acoustic Solitons on Distribution Functions of Background Plasma

F. M. Trukhachev[a, b, c, *], M. M. Vasiliev[a, b], and O. F. Petrov[a, b]

[a] *Joint Institute for High Temperatures, Russian Academy of Sciences, Moscow, 125412 Russia*
[b] *Moscow Institute of Physics and Technology (National Research University), Dolgoprudny, Moscow oblast, 141700 Russia*
[c] *Belarussian–Russian University, Mogilev, 212000 Belarus*
**e-mail: ftru@mail.ru*

Received June 17, 2022; revised July 7, 2022; accepted July 7, 2022

Abstract—Dynamics of an ensemble of ions of background plasma in the presence of ion–acoustic solitons in analyzed within the framework of the MHD model. Ion velocity distribution function perturbed by solitons is found. It is demonstrated that solitons transform the initial equilibrium ion distribution to the form similar to distribution of plasma containing an ion beam. Characteristic features of the perturbed ion distribution function corresponding to solitons of different amplitude are determined. The case of propagation of a cascade of solitons frequently observed in practice is analyzed.

Keywords: soliton, soliton currents, plasma distribution function
DOI: 10.1134/S1063780X2260075X

1. INTRODUCTION

Waves and instabilities play an important role in plasma dynamics. Analysis of influence of wave processes on distribution functions of background plasma currently represents one of the central physical problem. Indeed, on the one hand, such studies help developing kinetic theory of plasma [1] and the theory of nonequilibrium systems [2]. On the other hand, they can be used for diagnostic of plasma properties and development of new methods of plasma heating [3–6].

In this work, we present solution to the problem of perturbation of the background plasma distribution function upon propagation of ion–acoustic (IA) solitons. This problem was mentioned for the first time in study [7] aimed at analysis of electric currents generated in collisionless plasma by solitons of acoustic type. In particular, by using MHD models and the single-particle approximation, it was demonstrated that the IA solitons elicit unidirectional ion transport by a distance of several Debye lengths. The direction of ion transport for solitons characterized by positive polarity of potential (compression solitons) coincides with the direction of wave propagation. In the "cold" plasma model, velocity and, consequently, kinetic energy of ions turn out to be equal to zero before and after interaction with solitons (only position of ions in space changes). Ion velocity inside the soliton is positive (see also [8]). Such transport leads to the appearance of pulsed ion currents with a DC component. Such currents were referred to as the "soliton currents" [7] (see also [9–11]). Time resolution of current-measuring devices needed for detection of soliton currents should be on the order of the period of ion plasma frequency [9], which is not always achievable in practice [12, 13]. Soliton currents can have a substantial impact on plasma properties during the propagation of a large ensemble of solitons in it. Such situation is frequently observed in cosmic plasma [13–15]. Nonzero DC component of soliton currents indicates that the ion distribution function perturbed by solitons must be different from the Maxwell one. The importance of our analysis is underscored by the fact that solitons and nonlinear waves play an important role in modern plasma physics, which can be seen from a large number of studies in the fields of astrophysics [13–22], cosmology [23–25], nuclear fusion [26, 27], fundamental plasma physics [28], etc.

2. BASIC EQUATIONS

Let us find the profile of potential and other parameters of IA solitons. To this end, let us use a one-dimensional collisionless MHD model of plasma with cold ions and hot electrons [7]. The model includes normalized equations of motion and continuity for ions, a Boltzmann equation for electrons, and a Poisson equation that couples together populations of charged particles:

$$\frac{\partial v_i}{\partial t} + v_i \frac{\partial v_i}{\partial x} = -\frac{\partial \Phi}{\partial x}, \quad (1)$$

$$\frac{\partial n_i}{\partial t} + \frac{\partial n_i v_i}{\partial x} = 0, \quad (2)$$

$$n_e = \exp(\Phi), \quad (3)$$

$$\frac{\partial^2 \Phi}{\partial x^2} = n_e - n_i. \quad (4)$$

Here, n_e and n_i are the electron and ion density normalized to unperturbed density n_0, respectively; v_i is the ion velocity normalized to the ion–acoustic speed $C_s = (T_e/m_i)^{1/2}$; T_e is the temperature of electron population; m_i is the ion mass; $\Phi = e\varphi/T_e$ is the normalized potential of electric field of the wave; e is the elementary charge. Time t is normalized to ω_i^{-1}, where $\omega_i = \sqrt{4\pi n_0 e^2/m_i}$ is the ion plasma frequency, and spatial coordinate is normalized to Debye length $\lambda_D = \sqrt{T_e/4\pi e^2 n_0}$. In our model, $T_i = 0$, so that the condition necessary for existence of ion acoustic waves $T_e \gg T_i$ is fulfilled automatically. Let us consider the solution for the waves undergone all stages of evolution that propagate retaining constant amplitude, shape, and velocity V. Next, V is expressed in terms of Mach number as $M = V/C_s$ after normalization. Transforming to the reference frame moving with the wave and introducing new variable $S = x - Mt$, we can express normalized ion density in the form [7]

$$n_i(\Phi) = \frac{M}{\sqrt{M^2 - 2\Phi}}.$$

After that, the system of equations (1)–(4) can be reduced to a single Poisson equation given by [7]

$$\frac{\partial^2 \Phi}{\partial S^2} = \exp(\Phi) - \frac{M}{\sqrt{M^2 - 2\Phi}}. \quad (5)$$

Single integration of (5) with respect to Φ taking into account boundary conditions $d\Phi/dS = 0$ at $\Phi = 0$ yields an expression governing Sagdeev pseutopotential given by [7]

$$U(\Phi) = \left(1 - e^{\Phi}\right) - \left(M\sqrt{M^2 - 2\Phi} - M^2\right). \quad (6)$$

The dependence of $U(\Phi)$ for different values of M is presented in Fig. 1a. Roots Φ_0 correspond to the soliton amplitudes. It is evident that the amplitude grows with increase in their velocity M (see Fig. 4a in [7]). Soliton profile $\Phi(S)$ is described by solution to differential equation (6) that can be found either numerically or in the small amplitude approximation ($|\Phi_0| = 1$). In the latter case, expansion $U(\Phi) \approx A_2\Phi^2 + A_3\Phi^3$ is used, where $A_2 = \frac{1}{2M^2} - \frac{1}{2}$ and $A_3 = \frac{1}{2M^4} - \frac{1}{6}$. Analytical expression governing the profile of an IA soliton can be written in the form [7]

$$\Phi(S) \approx \Phi_0^* \operatorname{sech}^2\left(\sqrt{-\frac{A_2}{2}}S\right), \quad (7)$$

where $\Phi_0^* = -A_2/A_3$ is the soliton amplitude. Analytical expression (7) is an approximation and is valid for description of solitons with low amplitude ($\Phi_0 < 0.2$), which can be seen from Fig. 1b. It is also evident from the figure that $\Phi_0^* > \Phi_0$. However, $\Phi_0^* \to \Phi_0$ with reduction in the amplitude.

Knowing the soliton profile and parameters of plasma, we now turn our attention to analysis of the distribution function of particles.

3. ION VELOCITY DISTRIBUTION FUNCTION. ENSEMBLE AVERAGE

Distribution function of light hot electrons can be considered to be Maxwellian with high degree of accuracy. Therefore, let us limit our analysis to finding the distribution function of ions. We consider the distribution function in the form of velocity distribution function (velocity can be either positive or negative). The expression governing one-dimensional velocity distribution function can be presented in the form

$$f(v_i) = \frac{\Delta N}{N\Delta v_i}, \quad (8)$$

where v_i is the x-component of the velocity, ΔN is the number of particles with velocities falling in the range from v_i to $v_i + \Delta v_i$, and N is the total number of ions in the area under consideration. Let us make some comments:

Comment 1. In out model of cold plasma, all ions are assumed to be uniformly distributed in space and to have zero initial velocity. Initial position of ions in the phase space thus differs only by their position in space.

Comment 2. Ion velocity distribution in the absence of solitons can be described by a Delta function that represents the limiting case of a Maxwell distribution at zero temperature.

Comment 3. As we mentioned before, subcritical IA solitons perturb ion velocity only in their vicinity; in the process, ion velocity taking only positive values [7]. Therewith, ions are moved by several Debye lengths in the direction of the wave propagation. Ion motion leads to generation of ion currents that have pulse character and contain a DC component. Hence, the perturbed ion velocity distribution function must be asymmetric with respect to zero. Otherwise, the average velocity of ions, along with the constant component of the ion current, would also be equal to zero.

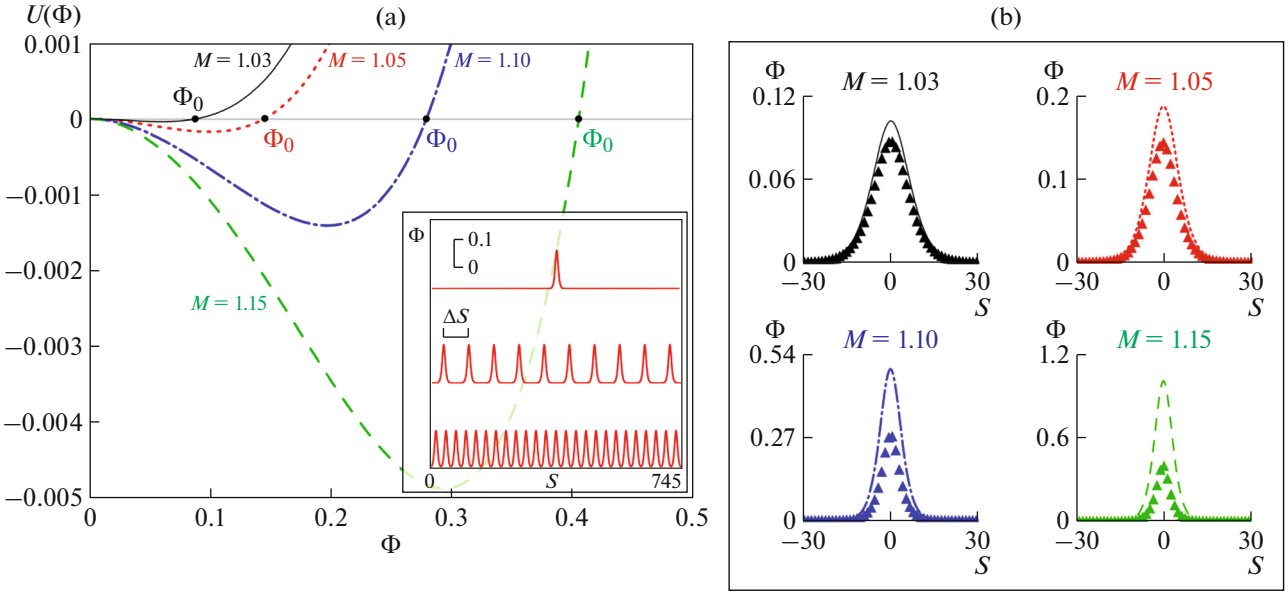

Fig. 1. (a) Sagdeev pseudopotential $U(\Phi)$ for different values of parameter M. Possible wave solutions to Eq. (5) in the form of an isolated soliton, a sequence of solitons with a period of ΔS, and cnoidal waves, respectively, are presented in the inset. Different initial conditions correspond to different types of solutions. The differences in initial conditions for an isolated soliton and a sequence of solitons are small, while soliton profiles in these two cases nearly coincide with each other. (b) Profiles of potential of the IA soliton at $M = 1.03$; $M = 1.05$; $M = 1.1$; $M = 1.15$. Analytical solutions are presented by solid, dotted, dash-dotted, and dashed lines, respectively. Corresponding numerical solutions are presented by symbols "▲".

Let us choose an ensemble containing N ions of background plasma that are uniformly distributed on a straight line along the x axis (Fig. 2). Suppose that the soliton at the initial moment of time was located to the left from the ensemble of ions so that it did not perturb dynamic parameters of the chosen ions. Soliton velocity is directed from left to right, i.e., toward the ensemble of ions. Let us find velocity distribution for the ensemble of ions at the moment of time when the soliton is located approximately in the center of the ensemble. Parameters of motion of singly charged ions in a stationary coordinate system can be found from the Newton's second law [9, 29]:

$$m_i\mathbf{a} = e\mathbf{E}, \tag{9}$$

where $\mathbf{E} = -\nabla\varphi$ is the self-consistent electric field of the soliton. Importantly, the ensemble of ions under consideration represents part of entire ion population involving in the self-consisted wave process. Therefore, motion of individual ions describes the motion of entire ion population. In the one-dimensional case, taking into account our normalizations, Eq. (9) can be rewritten in the form

$$\frac{d^2x}{dt^2} = -\frac{\partial\Phi}{\partial x}. \tag{10}$$

Function $\Phi(x, t)$ can be found in explicit form by using substitution $S = x - Mt$ in (7) or numerically (in the form of a table). Equation (10) holds for all ions of the ensemble under consideration. The differences consist only in initial conditions that describe the position of individual ions at the initial moment of time. Moreover, it is seen from Fig. 12a in [7] that trajectories of all ions are identical (the differences consist in spatiotemporal shift). The initial conditions are as follows:

(1) the number of ions in the ensemble is $N = 15$;

(2) the initial velocity of all ions of the ensemble is $v_i(0) = dx/dt = 0$;

(3) the initial positions of ions are: $x_1(0) = x_0$, $x_2(0) = x_0 + \Delta x, \ldots, x_N(0) = x_0 + \Delta x(N-1)$, where $x_0 = 30$ represents the initial position of the first particle of the ensemble, and $\Delta x = 3$ is the distance between adjacent particles;

(4) the initial position of soliton is $x_S(0) = 0$, and its velocity is $M = 1.05$ (the corresponding profile is illustrated in Fig. 1).

Equation (10) is solved by using the fourth-order Runge–Kutta method. The main phases of the process of interaction of an IA soliton with the ensemble of ions are illustrated in Fig. 2, namely, the initial state of the system (a), its state when the soliton is located at the center of the ensemble of ions (b), and the state when the soliton moves away from the ensemble (c).

Position of ions of the ensemble is shown by symbols "●", while initial position of particles is shown by symbols "○". For the sake of clarity, symbols "●" and "○" are separated vertically. Position of particles in the

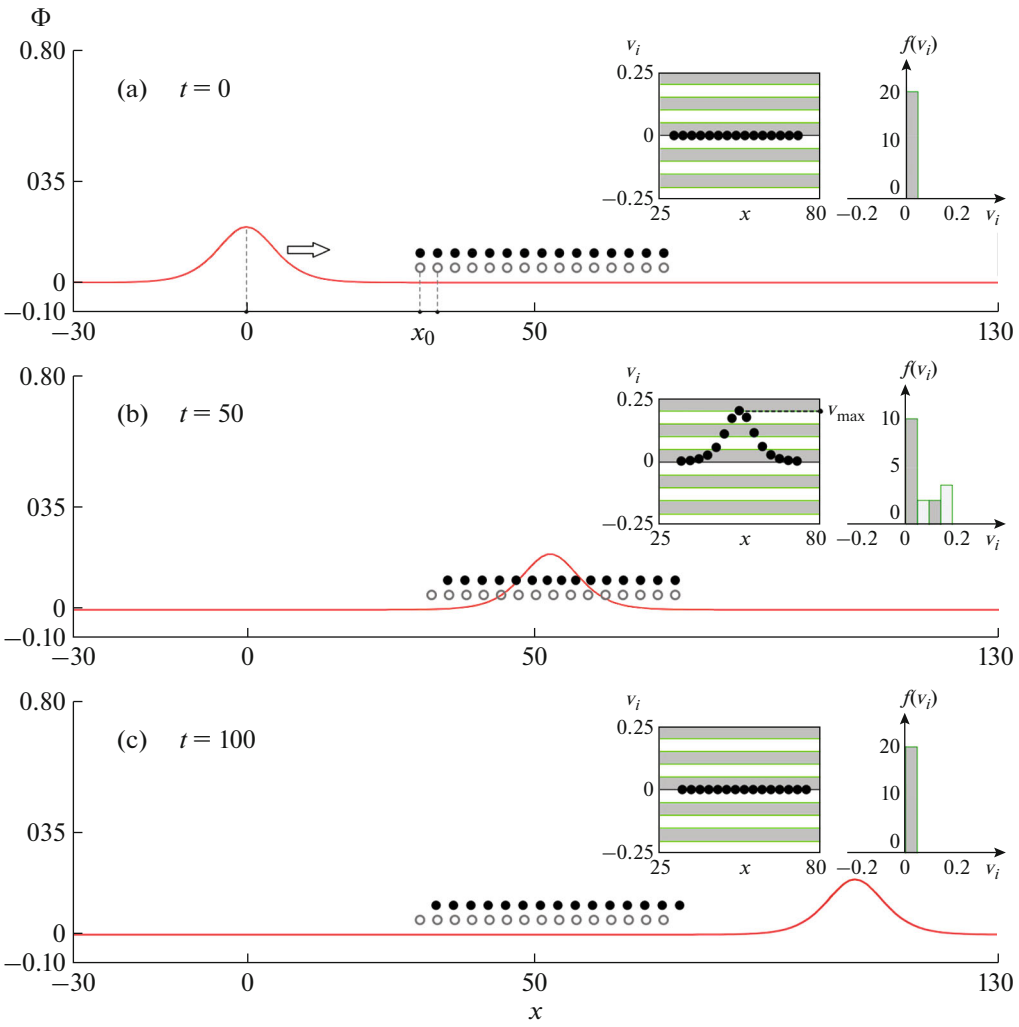

Fig. 2. Phases of IA soliton interaction with an ensemble of ions. Symbols "○" and "●" denote initial and current positions of ensemble ions, respectively. Symbols "○" and "●" are separated vertically for better view. (a) *Phase 1*, state of the system before interaction, initial velocity of ensemble ions equals zero; (b) *phase 2*, IA soliton reaches the center of the ensemble, ion velocity is nonzero; and (c) *phase 3*, soliton leaves the ensemble, ion velocity equals zero again, all ions shifted forward by a distance of several λ_D. Positions of particles in the velocity space (phase space), along with the distribution of ensemble ions with respect to projection of velocity, are presented in the insets.

velocity space (phase diagrams), along with histograms of velocity distribution $f(v_i)$, are presented in insets in Fig. 2. The velocity axis is divided into intervals of length $\Delta v_i = 0.05$. These intervals are used for finding discrete distribution function $f(v_i)$ calculated using expression (8).

It can be seen from Fig. 2a that all ions of the ensemble are at rest initially (phase 1), and their velocities are equal to zero. We noted above (comment 2) that their velocity distribution tends to a delta function in this case. A similar distribution is observed after soliton leaves the ensemble of ions (phase 3). Phase 3 differs from phase 1 only by position of ions that were shifted by the soliton by distance $\ell \sim 3\lambda_D$, while particle spacing and ion velocity take initial values of $\Delta x = 3$ and $v_i = 0$, respectively. The process of interaction of an isolated ion with an IA soliton was described in detail in [7, 9].

Phase 2 that can be considered as the active phase of the soliton–particle interaction is of special interest. At this phase, the soliton is located approximately in the center of the ensemble. It is evident from the inset in Fig. 2b that velocity of ions of the ensemble assumes nonnegative values in this case (i.e., $v_i \geq 0$). The ion velocity distribution can be easily found using expression (8). To this end, it is sufficient calculating the number of ions in each velocity interval $[v_i, v_i + \Delta v_i)$ (for convenience, adjacent intervals are filled with different color). It can be seen from the inset in Fig. 2b that the velocity distribution of particles has an asym-

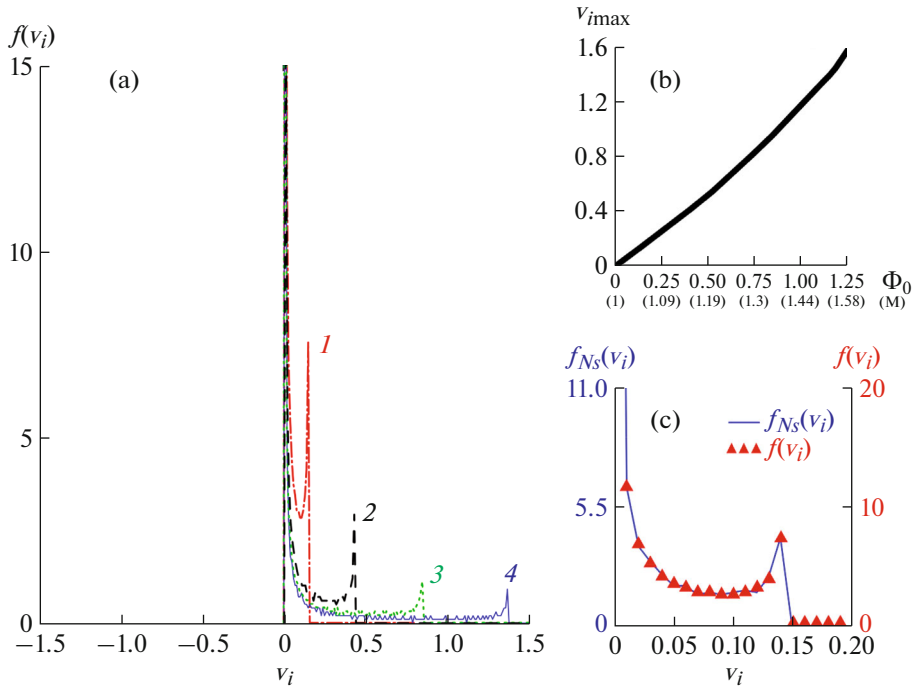

Fig. 3. Perturbed ion velocity distribution functions $f(v_i)$ (in phase 2) for large ion ensembles ($N = 1000$) for several values of Mach number: curve *1*—$M = 1.05$; *2*—$M = 1.15$; *3*—$M = 1.3$; and *4*—$M = 1.5$; other parameters of the simulation: (a) $\Delta x = 0.04$ and $\Delta v_i = 0.01$; (b) maximum velocity of ions inside the soliton $v_{i\max}(\Phi_0)$ as a function of its amplitude; and (c) perturbed distribution function calculated for the ensemble of solitons illustrated in the inset in Fig. 1a for the following parameters: $M = 1.05$, $N = 1000$, $\Delta x = 0.745$, and $\Delta v = 0.01$.

metric shape, which agrees with comment 3. In particular, $f(v_i) = 0$ at $v_i < 0$. However, $f(v_i) > 0$ in the interval of positive velocities $0 \le v_i < 0.2$. It is in this interval that velocities of ion interacting with the soliton fall into.

Obviously, the accuracy of obtaining function $f(v_i)$ will increase with increase in number N of particles in the ensemble, as well as upon reduction in increments Δx and Δv_i. Perturbed ion distribution functions for phase 2 for a relatively large ensemble of particles ($N = 1000$) and different values of Mach number (and, correspondingly, different soliton amplitudes Φ_0) are presented in Fig. 3. The following values of parameters are used in the calculations: $\Delta x = 0.04$; $\Delta v_i = 0.01$. The method of calculations is identical with the method of obtaining the data presented in Fig. 2, namely, Eq. (10) is solved N times for different initial positions of an ion. This procedure yielded a set of N discrete dependences $v_i(t)$. After that, time t at which the soliton was located approximately at the center of the ensemble of ions is fixed (e.g., $t = 50$ for the case illustrated in Fig. 2b). A one-dimensional array (a row) of size N that contained velocities of all ions of the ensemble at a given moment of time is thus obtained. The obtained array is processed using a simple algorithm that counted the number of particles in each interval of velocities $[v_i; v_i + \Delta v_i)$. Note that the numerical profile of the electric field of the soliton is used when solving Eq. (10), because expression (7) yields a large error at large values of Φ_0. Numerical profiles $\Phi(S)$ illustrated in Fig. 1b are found as a result of integration of Eq. (6) (or Eq. (5)) by means of the Runge–Kutta method. In the process, a nonzero root of equation $U(\Phi) = 0$ served as initial condition $\Phi(0) = \Phi_0$ for numerical solution of Eq. (6) (which is seen in Fig. 1a).

Let us analyze the obtained results. The shape of the ion velocity distribution function for all values of parameter M is characterized by two local maxima that we denote v_1 and v_2, respectively. The first maximum is located in the vicinity of zero (i.e., $v_1 = 0$) for any value of M. At the same time, the second maximum is located in the region of positive velocities. The first maximum is fundamental and is determined by unperturbed ions of the background. For the model under consideration, the first maximum is formed by ions not yet involved into interaction with the soliton and ions that had enough time to relax to equilibrium after interaction. In the absence of solitons, this maximum reduces to a delta function that describes an ion distribution function in an unperturbed state. Position of the second maximum of the distribution function shifts to the right with increase in soliton velocity M

(and its amplitude Φ_0). Diagrams presented in Fig. 3 allow drawing a conclusion that the second maximum corresponds to maximum velocity that ions can gain as a result of interaction with the soliton: $v_2 = v_{i\max}$. The value of $v_{i\max}$ is illustrated in inset in Fig. 2b. The dependence of $v_{i\max}(\Phi_0)$ is presented in Fig. 3b. It can be seen that the value of $v_{i\max}$ grows with increase in the soliton amplitude (and its velocity). For large-amplitude solitons, $v_{i\max} \to M$.

Normalization of the distribution function consisting in the traditional condition that $\int_{-\infty}^{\infty} f(v_i)\,dv_i = 1$ is an important aspect. In the discussed case, normalization of function $f(v_i)$ occurs naturally according to expression (8), namely, $\sum f(v_i)\Delta v_i = (\sum \Delta N)/N = 1$. In other words, normalization is carried out by dividing by number N of particles in the ensemble. The value of N determines the size of the area occupied by the ensemble in space. The size of the area can be found using relation $X = N\Delta x$. Results illustrated in Fig. 3a were obtained assuming that $X = 40\lambda_D$. In our simulation, soliton was completely contained inside area X, i.e., $D < X$, where D is the soliton width. When $D < X$ (preferably, with some margin), the shape of function $f(v_i)$ corresponds to that illustrated in Fig. 3a. The first maximum of distribution function $f(v_1)$ grows with increase in the area of simulation X, while the second maximum of $f(v_2)$ diminishes. This is because the number of unperturbed ions increases with increase in width X of the area of simulation. It can easily be demonstrated that the discrete distribution function reduces to a delta function when $X \to \infty$.

From practical point of view, the value of X is related to spatiotemporal resolution upon measurement of the distribution function of charged particles in plasma. Specific form of this relation depends on many factors and will not be discussed here.

It can be seen from Fig. 3a that the shape of the distribution function perturbed by the soliton is similar to the distribution function of plasma containing a beam (see, e.g., Fig. 1.17 in [30]).

4. DISCUSSION

Obtained results suggest that the influence of soliton on the distribution function of the background plasma is limited to the area where the soliton is located. This means that the described phenomenon requires having high spatiotemporal resolution upon its experimental investigation. An order of magnitude estimate of the required resolution was obtained in [7, 9] and was found to be at the level of several Debye length and several periods of the ion plasma frequency. The situation becomes substantially simpler when considering a group of solitons propagating one after the other. In this case, the requirements for the resolution are considerably relaxed, and it is sufficient measuring the distribution function using a much longer period of time for accumulation of information. As we mentioned above, the case of propagation of a group of solitons was frequently observed experimentally [13–15]. The phenomenon of large soliton ensembles (soliton gas) was also studied theoretically (see, e.g., [31] and references therein). Let us compare our results with the results already known. The case of propagation of a large group of solitons was analyzed within the framework of the MHD models in [7, 9, 10]. In this situation, the average soliton current turns out to be relatively high. Let us analyze the case of propagation of N_S identical solitons. Such a situation can be simulated either by summing soliton solutions shifted in space [32] or by numerically integrating Eq. (5) with proper initial conditions [7, 9]. We opted using the second approach. All characteristics of solitons correspond to Mach number $M = 1.05$. Initial conditions upon integrating Eq. (5) we chosen in the following form: $\Phi|_{S=0} = 1.2 \times 10^{-5}$; $d\Phi/dS|_{S=0} = 0$, so that the soliton period is equal to $T = 71$. In this case, the distance between centers of solitons can be found using a simple relation: $\Delta S = TM \approx 74.5$. The corresponding numerical solution is presented in the inset in Fig. 1a (in the middle). The situation at $N_S = 10$ corresponds to the one illustrated in Fig. 8 in [7]. Ion velocity distribution in entire interval of $\Delta S N_S = 745$ can be found using the algorithm described in Section 3. Let us denote the corresponding distribution function as $f_{N_S}(v_i)$. This function is plotted in Fig. 3c. Calculations are carried out using the following parameters: $\Delta x = 0.745$ and $\Delta v_i = 0.01$. It can be seen that, up to a constant (normalization) factor, function $f_{N_S}(v_i)$ corresponds to function $f(v_i)$ presented in Fig. 3a for $M = 1.05$. Knowing the velocity distribution function, the average current density can be found using expression [33, 34]

$$\mathbf{j} = q\int f(v)\,\mathbf{v}\,d\mathbf{v}, \tag{11}$$

where q is the charge of the particles. In the one-dimensional case and taking into account normalization factors, expression (11) governing the average density of ion current can be rewrite in the form $J_i = \int_{-\infty}^{\infty} v_i f_{N_S}(v_i)\,dv_i$, or

$$J_i = \sum_k (\Delta v_i k)\, f_{N_S}(\Delta v_i k)\,\Delta v_i \tag{12}$$

for the discrete case.

For parameters corresponding to Fig. 3c, we find that $J_i \approx 0.023$. With increase in the accuracy of discrete calculations (at $N = 4000$, $\Delta x = 0.18625$, $\Delta v = 2.5 \times 10^{-4}$ in particular), we find that $J_i \approx 0.026$. Calculated value agrees well with the results obtained in [7] independently using MHD models and within the framework of a single-particle approximation.

It can be expected that the second maximum will "smear out" if solitons in a group are not identical [31]. A logical continuation of the current research will be obtaining analytical expressions describing perturbed distribution functions of charged particles.

5. CONCLUSIONS

Using a one-dimensional MHD model of a two-component collisionless plasma and single-particle (Lagrange) approximation, we analyzed the ion distribution function perturbed by an ion–acoustic soliton or a group of solitons. Calculations were based on analysis of velocities of a large number of ions participating in the interaction with the soliton. It is demonstrated that the perturbed distribution function has the shape similar to that of plasma containing an ion beam, i.e., it is characterized by two maxima. The first one is fundamental and it is located at $v_i = 0$. This maximum is determined by ions that are far from the soliton at a given moment of time. The second maximum is located at $v_i > 0$. In the process, it lies in the subsonic region for solitons of low amplitude and in the supersonic region for solitons of high amplitude. The average density of ion current J_i induced by a group of solitons that was calculated using the distribution function agrees well with the results obtained within the framework of MHD models in [7, 9].

FUNDING

This research was supported by the Russian Science Foundation, project no. 19-12-00354.

CONFLICT OF INTEREST

The authors declare no conflicts of interest.

OPEN ACCESS

REFERENCES

1. Yu. L. Klimontovich, *Kinetic Theory of Nonideal Gases and Nonideal Plasmas* (Nauka, Moscow, 1975; Pergamon, Oxford, 1982).
2. I. Prigogine, *Introduction to Thermodynamics of Irreversible Processes* (Interscience, New York, 1961).
3. K. Stasiewicz, R. Lundin, and G. Marklund, Phys. Scr. **2000**, 60 (2000).
4. J. Seo, Y.-S. Na, and T. S. Hahm, Nucl. Fusion **61**, 096022 (2021).
5. I. B. Bernstein, J. M. Green, and M. D. Kruskal, Phys. Rev. **108**, 546 (1957).
6. A. B. Gurevich, Sov. Phys.–JETP **26**, 575 (1967).
7. F. M. Trukhachev, M. M. Vasiliev, and O. F. Petrov, High. Temp. **58**, 520 (2020).
8. C. R. Johnston and M. Epstein, Phys. Plasmas **7**, 906 (2000).
9. F. M. Trukhachev and A. V. Tomov, Cosmic Res. **54**, 351 (2016).
10. F. M. Trukhachev, A. V. Tomov, M. M. Mogilevsky, and D. V. Chugunin, Tech. Phys. Lett. **44**, 494 (2018).
11. F. M. Trukhachev, M. M. Vasiliev, and O. F. Petrov, in *Proceedings of the 18th International Workshop on Complex Systems of Charged Particles and Their Interactions with Electromagnetic Radiation, Moscow, 2022,* p. 59.
12. N. Dubouloz, J. J. Berthelier, M. Malingre, L. Girard, J. Covinhes,Yu.I. Gal'perin, D.V.Chugunin, M. Godefroy, G. Gogly, C. Guerin, J.-M. Illiano, P. Kossa, F. Leblanc, F. Legoff, T.M. Mularchik, et al., CosmicRes. **36** (1), 3 (1998).
13. J. S. Pickett, S. W. Kahler, L.-J. Chen, R. L. Huff, O. Santolik, Y. Khotyaintsev, P. M. E. Décréau, D. Winningham, R. Frahm, M. L. Goldstein, G. S. Lakhina, B. T. Tsurutani, B. Lavraud, D. A. Gurnett, M. André, et al., Nonlinear Processes Geophys. **11**, 183 (2004).
14. H. Matsumoto, H. Kojima, T. Miyatake, Y. Omura, M. Okada, I. Nagano, and M. Tsutsui, Geophys. Res. Lett. **21**, 2915 (1994).
15. S. R. Bounds, R. F. Pfaff, S. F. Knowlton, F. S. Mozer, M. A. Temerin, and C. A. Kletzing, J. Geophys. Res.: Space Phys.**104**, 28709 (1999).
16. J. D. Williams, L.-J. Chen, W. S. Kurth, D. A. Gurnett, and M. K. Dougherty, Geophys. Res. Lett. **33**, L06103 (2006).
17. F. Haas and S. Mahmood, Phys. Rev. E: Stat., Nonlinear, Soft Matter Phys.**92**, 053112 (2015).
18. G. S. Lakhina, S. Singh, R. Rubia, and S. Devanandhan, Plasma **4**, 681 (2021).
19. A. Mukherjee, S. P. Acharya, and M. S. Janaki, Astrophys. Space Sci. **366**, 7 (2021).
20. F. S. Mozer, J. W. Bonnell, E. L. M. Hanson, L. C. Gasque, and I. Y. Vasko, Astrophys. J. **911**, 89 (2021).
21. R. Jahangir and S. Ali, Front. Phys. **9**, 622820 (2021).

22. S. P. Acharya, A. Mukherjee, and M. S. Janaki, Nonlinear Dyn. **105**, 671 (2021).
23. A. E. Dubinov, S. K. Saikov, and A. P. Tsatskin, J. Exp. Theor. Phys. **112**, 1051 (2011).
24. M. N. Khattak, A. Mushtaq, and Z. Ehsan, Chin. J. Phys. **54**, 503 (2016).
25. A. E. Dubinov and X. I. Lebedeva, Chaos, Solitons Fractals **152**, 111391 (2021).
26. N. Dashtban, S. M. Motevalli, and T. Mohsenpour, Plasma Phys. Rep. **44**, 854 (2018).
27. F. F. Lu and S. Q. Liu, AIP Adv. **11**, 055112 (2021).
28. U. N. Ghosh, A. Saha, N. Pal, and P. Chatterjee, J. Theor. Appl. Phys. **9**, 321 (2015).
29. F. M. Trukhachev, M. M. Vasiliev, O. F. Petrov, and E. V. Vasilieva, Phys. Rev. E **100**, 063202 (2019).
30. L. A. Artsimovich and R. Z. Sagdeev, *Plasma Physics for Physicists* (Atomizdat, Moscow, 1979) [in Russian].
31. F. Carbone, D. Dutykh, and G. A. El, EPL **113**, 30003 (2016).
32. F. M. Trukhachev, M. M. Vasiliev, O. F. Petrov, and E. V. Vasilieva, J. Phys. A: Math. Theor. **54**, 095702 (2021).
33. I. V. Kulikova, Prikl.Fiz., No. 2, 27 (2020).
34. A. A. Vlasov, *Theory of Many-Particle Systems* (Gostekhizdat, Moscow, 1950) [in Russian].